A&A manuscript no.
(will be inserted by hand later)

Your thesaurus codes are:
03 (11.17.3, 11.19.1, 11.05.2, 11.12.2, 12.03.3 12.07.1)

ASTRONOMY AND ASTROPHYSICS

The bright end of the QSO luminosity function

Lutz Wisotzki

Hamburger Sternwarte, Gojenbergsweg 112, D-21029 Hamburg, Germany,
e-mail: lwisotzki@hs.uni-hamburg.de

Received ; accepted

Abstract. We have analysed the optical luminosity-redshift distribution properties of bright QSOs, using a new large sample from the Hamburg/ESO survey. The sample provides insight into the hitherto poorly sampled bright tail of the luminosity function, allowing to monitor its evolution with redshift up to $z \approx 3$. The slope increases significantly towards higher z, inconsistent with the predictions of pure luminosity evolution, but also with other recently proposed parameterisations. This phenomenon is opposite to what would be expected from gravitational lensing, showing that magnification bias does not significantly distort the QSO luminosity function within the redshift range covered. The space density of high-luminosity QSOs continues to increase up to the high-redshift limit of the survey, without indication of reduced evolution above $z \simeq 2$. The sample also permits an improved estimate of the local ($z \approx 0$) luminosity function of QSOs and bright Seyfert 1 nuclei, over the luminosity range $-27 \lesssim M_{B_J} \lesssim -20$. No evidence for a break or change of slope is found down to absolute magnitudes $M_{B_J} \simeq -20$.

Key words: Quasars: general – Galaxies: Seyfert – Galaxies: evolution – Galaxies: luminosity function – Cosmology: observations – Gravitational lensing

1. Introduction

The wide range of quasar luminosities, spanning altogether over four decades from low-activity Seyfert galaxies up to the most luminous objects in the universe found at high z, allows individual surveys to access only small portions of the luminosity-redshift-plane at given redshift. While at intermediate flux levels there are now many samples available, large uncertainties still exist at the faint and bright tails of the QSO luminosity function (QLF). The lack of good constraints for the bright end is particularly grave in the optical waveband, where the Palomar-Green Bright Quasar Sample (BQS; Schmidt & Green 1983) has been the only significant contributor for now 15 years, although ist is now well known to be substantially incomplete (Goldschmidt et al. 1992; Köhler et al. 1997).

The most widely quoted analysis of the quasar luminosity function is due to Boyle and collaborators (e.g., Boyle et al. 1988). who concluded that the evolution proceeds along increasing luminosity, with the simple scheme of 'pure luminosity evolution' (PLE) providing a statistically acceptable fit to their data. However, the Boyle et al. analysis had to rely on the BQS and was therefore affected by the incompleteness of that sample. Newer surveys sensitive to the brighter part of the QSO population have questioned the validity of the PLE picture. In a preliminary analysis of the LBQS, Hewett et al. (1993) showed that the PLE model predicts too few bright and too many faint low-redshift quasars. A similar conclusion was reached by Goldschmidt & Miller (1998) using the Edinburgh survey, by La Franca & Cristiani (1997) from a combined analysis of EQS and HBQS, and by Köhler et al. (1997) comparing their 'local' QLF with the PLE prediction.

For redshifts $z > 2$, the general view is that the evolution slows down considerably around $z \simeq 2$ and eventually reverses. The actual onset of this reversal is, however, not well constrained, and may well depend on luminosity. In the PLE model of Boyle et al. (1991), comoving space densities are roughly constant for redshifts $z \gtrsim 1.9$, while the results of Hewett et al. (1993) and Warren et al. (1994) suggest that space densities still increase up to $z \simeq 3$, although at a reduced rate, but drop precipitously thereafter. A marked decline in space densities towards higher z was also found by Schmidt et al. (1995). However, all these surveys sampled mainly intermediate-luminosity QSOs with $M_B \simeq -26$. For highest luminosities, $M_B \lesssim -28$, there is very little material available, and the few results so far are controversial. Irwin et al. (1991) claimed that there is no evidence for evolution at all, up to $z = 4.5$. This has been disputed by Kennefick et al. (1995), who obtain an order of magnitude lower space densities at $z = 4.3$ than Irwin et al. Resolving this controversy will require new wide-angle survey material; the first results from the just started Sloan Digital Sky Survey (Fan et al. 1999) indicate that data on high-luminosity QSOs in the very early universe will soon be available in substantial numbers.

In this paper we present the contribution of a new large sample of bright QSOs, drawn from the Hamburg/ESO survey (HES; Wisotzki et al. 1996, Reimers et al. 1996). This sample contains many of the most luminous quasars known and is suited to study the evolutionary properties at the bright part of the QLF over a wide range of redshifts. It is also the first

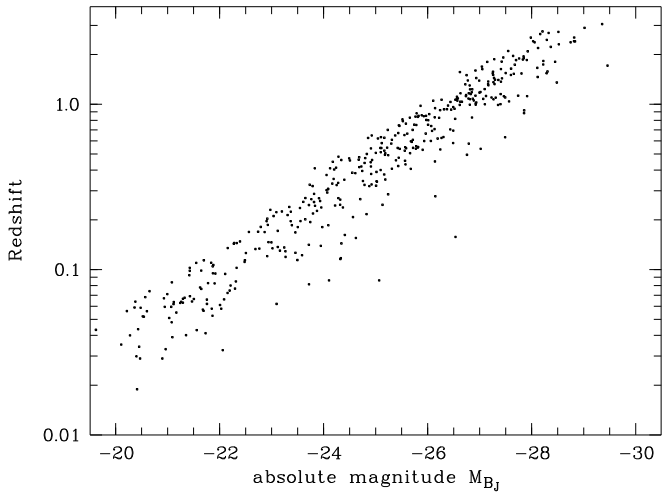

Fig. 1. Distribution of the 415 QSOs of the flux-limited HES sample over absolute magnitudes and redshifts.

quasar sample large enough to effectively *replace* the BQS, with higher completeness, photometric accuracy, and less affected by redshift-dependent selection biases. The main aim of this paper is to use the HES sample to derive constraints on the evolution of luminous QSOs. We do not attempt to compute new evolutionary models, as that would require merging the HES with other, fainter samples – a complication that we wish to avoid in the present paper.

2. Observational data

The Hamburg/ESO survey was initiated in 1990 as an ESO key programme, to perform a wide-angle search for bright QSOs in the southern sky. The survey uses objective prism plates taken with the ESO Schmidt telescope and digitised with the Hamburg PDS microdensitometer (for more details on the survey see Reimers & Wisotzki 1997; Wisotzki et al. 1999 – hereafter Paper 1).

The selection of QSO candidates from the database of digital spectra involves a multitude of selection criteria. Extensive follow-up spectroscopy conducted at ESO has allowed to construct a new flux-limited sample of 415 objects within the redshift range $0 \lesssim z < 3.2$, with optical magnitudes $B_J \lesssim 17.5$; a full discussion of the sample properties is given in Paper 1, of which only some essentials are summarised here. The sample was compiled from processing 207 HES Schmidt fields with complete follow-up spectroscopic identification down to well-defined flux limits. Each field has its own limiting magnitude depending on the quality of photographic plates and seeing. While one single Schmidt plate formally subtends over $\sim 5^\circ \times 5^\circ$, the *effective survey area* is reduced because of overlapping adjacent plates and loss of processable area. The total effective area $\Omega_{\rm eff}$ is $3700\,\mathrm{deg}^2$ for $B_J < 14.5$, and a monotonously falling function of magnitude for fainter objects. The uncertainties of optical photometry are generally smaller than 0.2 mag. All redshifts were determined from follow-up slit spectra, with typical continuum S/N ratios of $\gtrsim 20$, and for no object the assignment of an appropriate redshift was in doubt.

Due to its wide range of selection criteria and highly automated surveying procedure, the HES is less affected by redshift-dependent selection biases than many other optical surveys. In Paper 1 we give an extensive discussion of the completeness for this sample; the central points are summarised as follows:
(1) The redshift distribution does not show evidence for significantly enhanced or reduced selection efficiency in certain redshift regions.
(2) More than 99 % of the previously known QSOs located within the survey area and above the flux limits were recovered.
(3) QSOs within the usual range of spectral properties are always selected.
(4) The surface density of bright QSOs as measured in the HES is higher by a factor of 1.5 than in the BQS, and fully compatible with other recent quasar surveys.

Given apparent magnitude B_J and redshift z, absolute magnitudes M_{B_J} of the QSOs were estimated using the usual formula $M_{B_J} = B_J + 5 - 5\log d_L(z) + A + K(z)$, where $d_L(z)$ is the 'luminosity distance' in an expanding Friedmann universe, computed with the relation given by Terrell (1977). We adopted $H_0 = 50\,\mathrm{km\,s^{-1}\,Mpc^{-1}}$ and $q_0 = 0.5$ to specify the cosmological model. For the extinction term A, only attenuation by Galactic dust has been assumed, and the values of A_{B_J} were estimated from H I column densities as described in Paper 1.

Somewhat more complex is the situation for the K term: Although quasar spectra have often been approximated by simple power laws $f_\nu \propto \nu^\alpha$ with adopted mean spectral index α between -1 and -0.3, actual spectral energy distributions are more complicated than this. We have recently determined a new K correction as a function of redshift that results in luminosities lower by 0.4 mag for high-z QSOs, compared to previously published relations (Wisotzki 1999), and we adopt that new $K(z)$ relation for the present paper. The reader should be alert that the space densities derived in the next section are therefore shifted towards lower luminosities, relative to what can be found in the literature. However, whenever comparisons with the results of earlier workers are carried out in this paper, in particular with parametric descriptions of the QLF and its evolution, we use the appropriate original $K(z)$ relations employed by others. The qualitative conclusions of this paper do not depend on the details of the adopted K correction.

Fig. 1 shows the distribution of sources over absolute magnitudes and redshifts. At $z < 0.1$, the majority of objects would usually be called Seyfert 1 galaxies rather than QSOs, but at all other redshifts there is no ambiguity of this sort, the HES always sampling the optically brightest parts of the known quasar population.

3. Luminosity functions

Space densities at given absolute magnitude were computed in bins of redshift, and luminosity for the binned differential

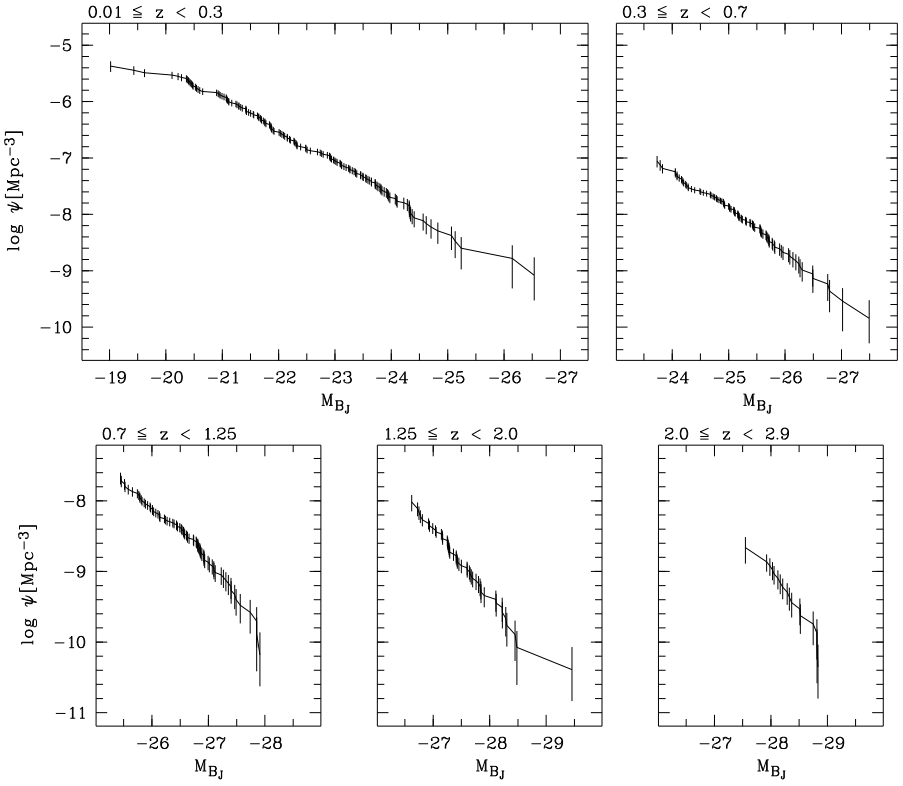

Fig. 2. The cumulative quasar luminosity function determined from the HES sample for five adjacent redshift shells. Each panel shows the result for one redshift domain, including error bars estimated from Poisson statistics.

form, using the $1/V_{\rm max}$ estimator (Felten 1976). Five redshift intervals were chosen to represent the evolution of the bright end of the QLF with cosmic time, with boundaries $z = 0.0$–0.3, 0.3–0.7, 0.7-1.25, 1.25–2.0, and 2.0–2.9. These intervals correspond to approximately equal steps in $\log(1+z)$ which is the cosmic time variable in the PLE model of Boyle et al. (1991), from where the above set of intervals was adopted. The lowest ($z = 0$–0.3) interval is not common in quasar evolution studies in the optical (see below), but has been added for this analysis.

Fig. 2 displays the luminosity function, in cumulative form, for each shell separately. As discussed by Hewett et al. (1993), this way of representing a luminosity function has considerable advantages over the conventional approach to bin the data in absolute magnitude: The contribution of each object is easily made apparent, the complicated weighting within the luminosity bins needs not be corrected for, and the full range of the data can be displayed without 'incomplete bin' edge effects. However, the data are still binned in redshift and the constructed luminosity functions therefore do not represent the QLF at specific epochs, but at 'mean' epochs that vary with luminosity (a form of Malmquist bias). In particular, in the presence of strong positive evolution, the apparent QLF for any given redshift shell will appear considerably flatter than the intrinsic QLF. The statistical test procedures employed below are not affected by this bias. In the following we comment briefly on the observed properties of each of the subsets.

$z < 0.3$: The local ($z \approx 0$) universe is the only domain where the full range of luminosities is technically accessible to a single flux-limited survey. The HES is the first optical quasar survey capable of fully exploiting this option, being specifically designed to reduce selection biases due to the presence of extended galaxy envelopes. This has already yielded a first estimate of the local QLF based on a small subsample of the HES (Köhler et al. 1997). The present sample of 160 objects with $z < 0.3$ increases the number of 20 'local QSOs' used by Köhler et al. by almost an order of magnitude, allowing a much more accurate assessment of QLF shape and slope. The local luminosity function is discussed further in Sect. 5 below.

$0.3 < z < 0.7$: This shell is equal to the 'low-redshift' regime of most other optical quasar surveys. Host galaxies are visible only in exceptional cases, due to the $(1+z)^4$ surface brightness dimming and the steep K correction for galaxy spectra in the B_J band. For $z < 0.5$, quasar spectra are generally extremely blue and easily separated from their UV colours; around $z \simeq 0.6$, the short-wavelength end of the 'little blue bump' causes quasar colours to be somewhat redder, but it is shown in Paper 1

that there is no evidence for a significantly reduced degree of completeness in the HES sample in this redshift range.

$0.7 < z < 1.25$: The redshift distribution seems to have a local maximum around $z \simeq 1.1$, but this is unlikely to be a positive selection bias: There are no strong emission lines visible (only C III] λ1909 which is often just barely detected), and neither the colour dependence of z nor the K correction have discernible features at this redshift. The most probable interpretation is that of a statistical fluctuation.

$1.25 < z < 2.0$: The bright end of the QLF in this shell is dominated by the exceptionally luminous QSO HE 0515−4415. In this redshift range, the total number of QSOs predicted by the B91 model is consistent with what is observed in the HES; however, there is a tendency that the number of fainter objects is predicted too high. This trend is continued, even stronger, in the LBQS as noted by Hewett et al. (1993), and it is also visible in the HBQS (La Franca & Cristiani 1997), and it is therefore likely that not incompleteness of the data, but an overprediction of the PLE model causes the discrepancy.

$2.0 < z < 2.9$: The high-redshift range of the present HES sample is still only sparsely populated. Up to $z \simeq 2.6$, the HES selection criteria are predominantly sensitive to continuum properties. Although Lyα is generally detected as a strong emission line from $z \gtrsim 1.8$ onward, the broad range of colour criteria employed in the HES ensures that *all* of the $z < 2.6$ QSOs in the sample are in fact colour-selected (cf. Paper 1), thus avoiding the strong biases associated with emission line detection. The expected quasar colours as functions of z show a strong maximum of UV excess around $z \simeq 2.1$ – therefore the decrease of numbers when passing the $z = 2$ mark cannot be related to selection effects.

At **$z > 2.6$**, the QSOs were generally found by feature-detection algorithms, depending on the presence of a strong Lα emission and/or a pronounced spectral break at the onset of the Lyman forest. Both features are common but not *necessarily* strong, making it hard to quantitatively assess the degree of (in)completeness. Another difficulty is the increasingly ill-defined K correction, with intergalactic Lyα forest absorption adding to the uncertainty of spectral energy distribution. The number of objects in the sample should be, at any rate, considered as a *lower limit* to the number expected for a 'perfect' sample limited only by B_J magnitude.

In Fig. 3 all data have been combined into one frame, presented in the traditional binned differential form. The HES provides substantial improvement over previous surveys in covering the bright end of the QLF at all redshifts $z \lesssim 3$, plus a full construction of the important *local* luminosity function. For comparison, the dotted line in Fig. 3 shows the differential QLF, integrated over the appropriate redshift ranges, from the Boyle et al. (1991) PLE model.

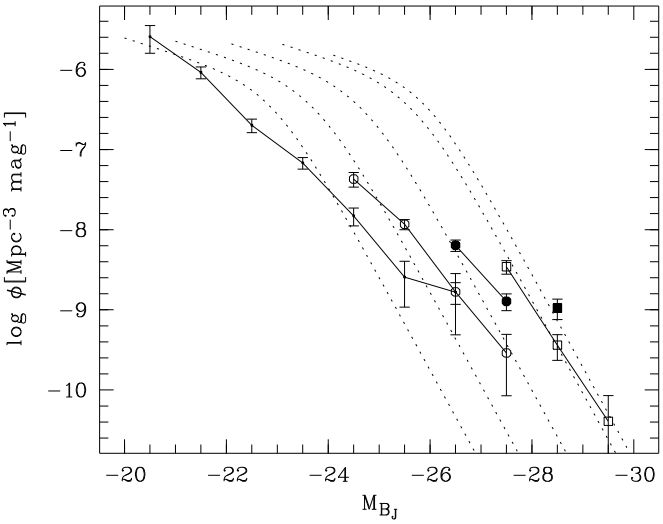

Fig. 3. Evolution of the differential QLF in bins of 1 mag with redshift. The redshift shells are the same as in Fig. 2, from left to right. The dotted line shows the prediction of the Boyle et al. (1991) PLE model.

4. Constraints on parametric models

4.1. Pure luminosity evolution

By combining the ∼ 400 QSOs from the AAT multifibre survey with a set of other, smaller quasar samples – in particular the BQS at the bright end –, Boyle et al. (1988) suggested that the quasar luminosity function can be approximated as a (logarithmically) shape-invariant double power law, merely shifted in luminosity by an offset governed through a redshift-independent evolution parameter $k_L \approx 3$–3.5. In a later analysis, Boyle et al. (1991; hereafter B91) substantiated this claim and extended the PLE model up to $z = 2.9$, albeit with the introduction of an additional parameter $z_{\max}$ above which the comoving space densities were kept constant.

Comparing the prediction of the specific parametric model of B91 with the empirical LF estimates based on the new HES sample (Fig. 3) reveals substantial discrepancies at most redshifts:

- At low and intermediate z, there is a significant excess of high-luminosity QSOs over the PLE prediction.
- At low redshifts, there are less intermediate-luminosity QSOs than demanded by PLE.
- The characteristic 'break' observed at high z does not appear in the local ($z < 0.3$) QLF.
- The QLF is much steeper at high redshift.
- There is evidence for continued evolution after $z > 2$.

Most of these discrepancies, in particular the feature of a relatively flat low-redshift QLF, were already detected in previous surveys (Hewett et al. 1993; Miller et al. 1993) and are clearly not artefacts of the HES selection procedure; the HES confirms these findings with high significance. Because the actual low-z QLF is flatter than the PLE prediction, discrepancies show up most prominently at the highest luminosities. With its large effective area and the luminosity range probed, the HES provides considerably improved statistical coverage to test the validity of the PLE parametrisation. A two-dimensional Kolmogorov-Smirnov test (Peacock 1983) applied to the joint

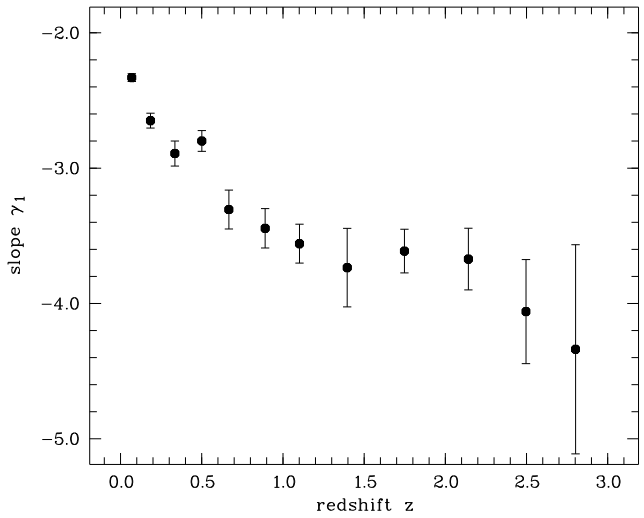

Fig. 4. Variation of the bright-end slope γ_1 with redshift.

distribution of (z, M) pairs yields a formal acceptance probability of $P = 10^{-7}$ for the redshift range $0.3 < z < 2.2$, and $P = 10^{-16}$ for the whole definition interval of the HES, $0 < z < 3.2$, so the B91 model is rejected with very high confidence.

An essential feature of all PLE models is the fact that the slope at the bright end of the QLF, γ_1, is necessarily constant. Fig. 3 shows that except for the $z < 0.3$ shell, the HES objects are always located on the steep part of the QLF, well beyond the ubiquitous 'break'; this will be so for all realistic PLE models. A good test for the validity of PLE models in general can be made by monitoring the bright-end slope of the QLF as a function of z. To this purpose we have fitted straight lines to the cumulative logarithmic LF within each redshift shell (i.e., assuming a power law). The result is shown in Fig. 4, where $\gamma_1(z)$ is resolved into redshift bins of $\Delta\log(1+z) = 0.05$. Although Malmquist bias and evolution within the shells tend to make the measured slope at given z somewhat flatter than the *intrinsic* one, the bins are small enough to ensure that this bias is almost negligible.

The trend for the bright-end slope to become flatter with decreasing redshift is very obvious, confirming the earlier conjecture by Goldschmidt & Miller (1998), with significantly improved redshift resolution. Fig. 4 also shows that this trend is confined to the redshift regime $z \lesssim 1$, while for $z > 1$ the slope is consistent with being constant at $\gamma_1 \simeq -3.7$, approximately equal to the value of γ_1 in most PLE fits (B91; La Franca & Cristiani 1997). Fig. 4 may be taken to furthermore suggest that the QLF steepens again after $z > 2$, but that is not statistically significant.

This test demonstrates that the basic assumption of all PLE models – a redshift-invariant QLF shape – is in conflict with observations, independently of the details of the parametrisation. The bright end of the quasar luminosity function undergoes a gradual transformation, becoming flatter with cosmic time.

4.2. Luminosity-dependent luminosity evolution

In a recent attempt that includes several sets of new survey material come available in the 1990s, La Franca & Cristiani (1997) modelled the QLF with a 'luminosity-dependent *luminosity* evolution' (LDLE) scheme, by equipping the PLE formula of Boyle et al. with an additional term to produce a flatter QLF at low redshift while maintaining the PLE description for higher redshifts. We have subjected their model (including the correction from La Franca & Cristiani 1998) to similar tests as the Boyle et al. model, with the following results: (1) There is very little difference in performance between LDLE and PLE for $z \gtrsim 1$. (2) The bright end slope γ_1 decreases (by absolute value) towards lower redshifts as demanded by the observations, but the number of luminous QSOs is *over*predicted. (3) Below $z \simeq 0.4$ the LDLE formalism assigns strongly *negative* evolution to the most luminous QSOs, producing an almost flat ($\gamma_1 = -1$) local luminosity function, which is of course incompatible with all available data. In conclusion, the LDLE scheme as proposed by La Franca & Cristiani does not resolve the shortcomings of PLE, and it is completely inadequate for the low-redshift domain.

4.3. Pure density evolution

Although pure density evolution (PDE) is the oldest and intuitively simplest form to parameterise an evolving luminosity function, it has been ruled out by several independent investigations. The argument is usually based on the counts of faint QSOs at high redshifts, which are observed to be much rarer than predicted by PDE. Even if faint QSO surveys are assumed to be substantially incomplete, a stringent limit is set by the measured intensity of the diffuse extragalactic soft X-ray background (Marshall et al. 1983). In a preliminary analysis of a composite ROSAT-selected AGN sample, Hasinger (1998) recently challenged the unequivocal rejection of the PDE concept, claiming that simple density evolution in fact provided a much better fit to the data than PLE. This claim has meanwhile been qualified (Miyaji et al. 1998; see below), but the performance of PDE with these new samples seems indeed surprisingly good.

While a detailed discussion of the similarities and differences between optically and X-ray selected samples is clearly outside the scope of this paper, it may be worthwhile to investigate the merits of PDE for the bright HES sample. Fitting a one-parameter PDE model to the data is simple: We use the modified variable $V'/V'_{\rm max}$ defined as the density-weighted volume integrals, $V' = \int \rho(z)\,dV$, where $\rho(z)$ is the density evolution function. Adopting the customary form for $\rho(z) = \rho(0)\,(1+z)^{k_D}$, k_D is varied until the sample average of $V'/V'_{\rm max}$ reaches 1/2. Based on the new K correction and using the full HES sample within $0 < z < 3.2$, this yields $k_D = 5.35$, thus a much smaller value than obtained in earlier fits based on fainter samples, but very similar to the X-ray value of Hasinger (1998). The distribution of $V'/V'_{\rm max}$ is also consistent with being uniform within [0,1]. However, this is only a necessary and not a

sufficient condition; the two-dimensional KS statistic yields a formal acceptance probability of $P = 10^{-17}$. For the first time, PDE can be significantly rejected from a bright QSO sample alone, *without any reference to faint QSO counts*. The reason is, of course, again the steepening of the bright QLF part towards higher redshift, leading to incompatible QLF shapes at low and high z. Note that although the $z \simeq 0$ and the $z \gtrsim 2$ QLF sections as seen in the HES do not overlap in luminosity, there is sufficient dynamic range at intermediate redshifts to monitor the steepening slope at given M_{B_J}.

4.4. Luminosity-dependent density evolution

A luminosity function changing with cosmic time can be always be described by the general concept of luminosity-dependent density evolution (LDDE). Concentrating on the more luminous part of the QSO population, Schmidt & Green (1983) proposed a specific LDDE scheme in which the more luminous QSOs undergo stronger evolution. (Note that this is not necessarily in conflict with the principles of PLE, which could be translated into an equivalent LDDE formalism.) However, in the Schmidt & Green picture, the QLF becomes successively steeper at smaller redshift, opposite to what is observed in the new samples.

A related approach was followed by Miyaji et al. (1998), accommodating the proposed density evolution of soft X-ray selected AGN (Hasinger 1998) with the constraints set by the X-ray background. In their formulation, the density evolution index $k_D(L)$ is smallest on the low-luminosity tail of the QLF; above a certain luminosity threshold, the index remains constant. The latter feature implies that directly transfering this model to the evolution of optically selected QSOs would result in the same conflicts as for the case of PDE discussed in the preceeding subsection. The specific merits of the Miyaji et al. LDDE model are in the low-luminosity regime, where the HES yields *no* constraints on the evolution rates, apart from the local luminosity function.

While a single survey such as the HES provides insufficient coverage of the Hubble diagram to allow new parametric models to be developed, it seems safe to conclude from the present data that only a rather complex luminosity-dependent evolution scheme will be capable to reproduce all observed features, making quasar evolution more complicated than previously thought.

5. The local luminosity function

The basic results of our earlier analysis of the local QLF (Köhler et al. 1997; hereafter K97) were: (1) The number of high-luminosity low-redshift QSOs has previously been underestimated. (2) The local QLF does not display any evidence of a break or significant change of slope at absolute magnitudes $M_{B_J} \lesssim -20$. The new HES sample improves the K97 data by a factor of 6 in covered area and by a factor of 8 in sample size. Both above mentioned results are confirmed in the present paper, although the discrepancy in number counts is less extreme than found in the K97 sample. However, considering the error bars, the results of the two analyses are fully compatible.

A new feature needing corroboration is the apparent flattening of the local QLF at luminosities fainter than $M_{B_J} \simeq -20$, apparent in Fig. 2. Note that it is based on only 3 sources with $M_{B_J} > -20$, thus the statistical significance of the feature is very low. We are currently investigating this part of the local QLF in more detail, including a dedicated treatment of host galaxy influences and including the transition to low-level AGN in nearby galaxies. For the present discussion we concentrate on objects with $M_{B_J} < -20$. Even for these, host galaxy contributions to standard isophotal magnitudes would be non-negligible. To avoid this effect, the HES magnitudes were measured over effective apertures of the size of the seeing disk, so the absolute magnitudes do not correspond to *total*, but effectively to *nuclear* luminosities; even large and bright host galaxies do not contribute with more than their seeing-convolved central surface brightness to the measured flux. Thus, while the measured magnitudes are not individually corrected for host galaxy contributions as it was the case in K97, they are nevertheless dominated by the active nuclei, not by the galaxy hosts.

The accurate determination of the local luminosity function of QSOs and Seyfert nuclei is an important, but also a difficult task. In addition to the challenge of generating unbiased samples, there are several problems to be overcome: Disentangling the contributions of nuclei and hosts to the measured luminosity is a problem not only in the optical domain, but also at X-ray wavelengths (Lehmann et al. 1998). A further complication arises from the probable bifurcation of the AGN population into a Seyfert 1 and a Seyfert 2 branch. These points need to be addressed before a meaningful physical interpretation of the local QLF can be made.

6. The most luminous QSOs at high redshift

6.1. Evolution of space densities

The substantial uncertaintes in the present knowledge of quasar evolution at redshifts $z > 2$ are mostly related to the increasing difficulties of obtaining sizeable well-defined flux-limited samples. The traditional UV excess method based on $U - B$ colours breaks down at $z = 2.2$ where the Lyα emission line is redshifted into the B band; multicolour techniques are capable of reaching higher z, but with the penalty of a complicated redshift-dependent selection function. Photographic objective prism surveys such as the LBQS and the HES, on the other hand, perform quite well up to $z \simeq 3$, but become rapidly incomplete towards $z = 3.4$ where Lyα moves out of the detector bandpass (see also Sect. 3). While the usefulness of the HES sample for space density estimation is therefore limited to $z \lesssim 3$, this is just the redshift region where most previous workers located the maximum of quasar activity. Furthermore, multicolour surveys show greatly reduced performance in this z range, including the forthcoming SDSS (Fan 1999).

While at low redshift the sampled luminosity range of a flux-limited survey depends sensitively on z, this dependency

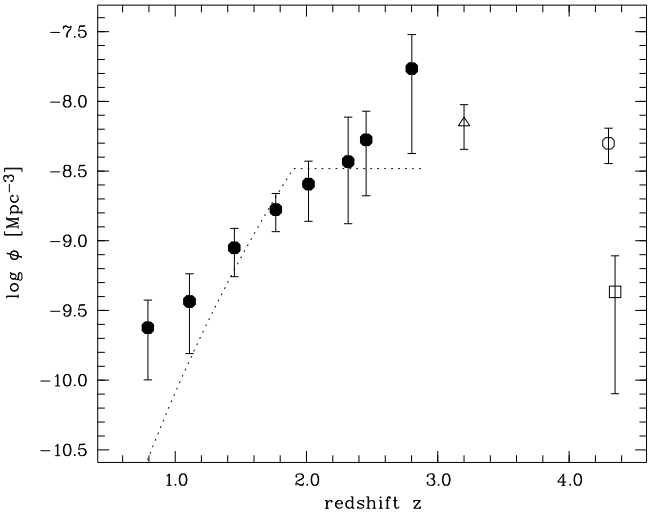

Fig. 5. Evolution of the integrated space density for QSOs with $M_B < -28$. The filled symbols show the values computed from the HES, the dotted line delineates the prediction of the B91 PLE model. Open symbold indicate the available higher redshift measurements for this luminosity regime (triangle: from Hewett et al. 1993; circle: Irwin et al. 1991; square: Kennefick et al. 1995).

is much weaker towards higher redshift, and here it is possible to trace quasar space densities *for given luminosity* over a wide redshift range. The HES provides appropriate data material to apply this to the rare species of very high luminosity QSOs, following their evolution up to $z \simeq 3$.

Fig. 5 shows the evolution of integrated comoving space density for $M_{B_J} < -28$ over several disjoint redshift bins. Beyond $z > 2.5$, even the faintest HES quasars are more luminous than this. The last plotted value is therefore based on a linear fit to the (logarithmic) cumulative luminosity function in the corresponding bin, extrapolated to $M_{B_J} = -28$. This increases the uncertainty, but does not bias the estimate. Recall also that QSO selection gets increasingly difficult close to the HES high-redshift limit, so that the true space density for this last point will be even higher.

The steady increase in space densities, up to the highest redshifts sampled, is remarkable. In particular, there is no indication for a turnover or only a slowing down of evolution. Unless the space density as a function of redshift shows an extremely narrow peak just below $z = 3$ – which would still be consistent with our data, considering the error bars –, we conclude that the maximum space density has almost certainly not yet been reached by our survey and must be located well beyond $z = 3$. This is in marked contrast to the general notion that the maximum of quasar activity occurs at $z < 3$ (e.g., Schmidt et al. 1995; Shaver et al. 1996). Two possible interpretations are conceivable:

(1) The maximum of quasar activity might depend on luminosity, in the sense that high-luminosity objects have a maximum shifted towards higher redshifts. Only three published surveys can provide meaningful additional datapoints for Fig. 5: The estimate for $3 < z < 3.4$ from the LBQS (Hewett et al. 1993) which is almost certainly only a lower limit; the $z > 4$ survey from Irwin et al. (1991), and the similar sample from Kennefick et al. (1995). None is in direct conflict with the HES data, but the high space density claimed by Irwin et al. (1991) seems to be joining particularly well with the HES. However, the origin of the discrepancy between the results of Irwin et al. and Kennefick et al. – based on partly the same objects – is not sufficiently understood. Kennefick et al. suggested that different adopted *K* corrections may be responsible, but this has not been confirmed so far.

Additional support for a stronger evolution of high-luminosity QSOs comes from the analysis of Warren et al. (1994): although their survey does not reach the luminosity range in question, their adopted luminosity evolution model in which only the bright part evolves can be extrapolated to evolution rates around $z \simeq 2$–3 that are quite compatible with the HES data.

If it should prove correct that high-luminosity QSOs continue to show positive evolution where the space densities of their lower luminosity counterparts already turn over, this has substantial consequences for cosmogony and galaxy formation scenarios. High luminosity presumably implies host galaxy mass (in analogy to the confirmed such relation at low redshifts, cf. McLeod & Rieke 1995). This would impose significant constraints on theories for the formation of very massive structures in the early universe.

(2) Incompleteness of fainter QSO surveys provides an obvious alternative explanation. Several recent deep surveys found high-redshift QSOs in larger numbers than anticipated (Miyaji et al. 1998; Wolf et al. 1999), although intercomparisons are difficult as each survey samples a different luminosity regime, and the statistics are still very poor.

6.2. Gravitational lensing

Statistical analyses based on optical quasar surveys can suffer from biases quite similar to those present in low-redshift QSO host galaxy studies: Systematic rejection of non-pointlike sources, a property of most surveys, invariably leads to missing large-separation lenses. The HES avoids this selection bias, and since since it samples the region of the QLF where 'magnification bias' (Turner 1980) is expected to be most effective, it is well suited as a testing ground for lensing statistics. While a full investigation of this subject is beyond the scope of this paper, we can make a few qualitative inferences on the effects of lensing onto the observed luminosity function.

The principal result of 'magnification bias' is to create a flatter observed QLF, compared to the intrinsic one. It can be shown that the effect is noticeable only when the QLF slope is steep (e.g., Schneider et al. 1992). As the optical depth for gravitational lensing increases with *z*, the magnification bias is expected to be stronger for sources at higher redshift. Under the assumptions of an intrinsically constant QLF slope and magnification bias being a dominant effect, we should observe

a bright end of the QLF that flattens with increasing redshift, opposite to what is actually observed. This does not exclude that there might be *some* influence of lensing on the observed luminosity function, but the observations constrain magnification bias to be of very minor importance for the QLF as a whole up to $z \simeq 2$. This is consistent with the fact that only ~ 1 out of 100 QSOs with $M_V < -28$ shows discernible image splitting due to lensing (Surdej et al. (1993).

7. Conclusions

The analysis of a new sample of very bright QSOs has shown that quasar evolution is more complex than generally assumed. The Hamburg/ESO survey provides insight into otherwise rarely sampled regions of the luminosity-redshift plane, enabling a direct assessment of the local luminosity function, and to probe the evolution of the bright part of the QLF up to $z \simeq 3$. While the high-redshift QLF has a very steep high-luminosity tail, the low-redshift QLF approaches towards a simple power-law form with rather flat slope. No simple 'pure' evolution scheme based on a shape-invariant QLF is capable of reproducing this transformation. Future analyses of large composite samples covering a wide range of luminosities are required to show if appropriate parametric descriptions can be found that are consistent with this behaviour.

References

Boyle B. J., Shanks T., Peterson B. A., 1988, MNRAS 235, 935
Boyle B. J., Jones L. R., Shanks T., et al., 1991, The Space Distribution of Quasars, ed. D. Crampton, ASP Conf. Ser. 21, 191
Fan X., 1999, AJ, in press, astro-ph/9902063
Fan X., Strauss M. A., Schneider D. P., et al., 1999, AJ, in press, astro-ph/9903237
Felten J. E., 1976, ApJ 207, 700
Goldschmidt P., Miller L., 1998, MNRAS 293, 107
Goldschmidt P., Miller L., La Franca F., Cristiani S., 1992, MNRAS 256, 65p
Hasinger G., 1998, Astron. Nachr. 319, 37
Hewett P. C., Foltz C. B., Chaffee F. H., 1993, ApJ 406, L43
Irwin M., McMahon R. G., Hazard C., 1991, in: The Space Distribution of Quasars, ed. D. Crampton, ASP Conf. Series 21, 117
Kennefick J. D., Djorgovski S. G., de Carvalho R. R., 1995, AJ 110, 2553
Köhler T., Groote D., Reimers D., Wisotzki L., 1997, A&A 325, 502
La Franca F., Cristiani S., 1997, AJ 113, 1517
La Franca F., Cristiani S., 1998, AJ 115, 1688 (Erratum)
Lehmann I., Hasinger G., Schwope A. D., Boller T., 1998, Highlights in X-ray Astronomy, in press, astro-ph/9810214
Marshall H. L., Avni Y., Tananbaum H., Zamorani G., 1983, ApJ 269, 35
McLeod K. K., Rieke G. H., 1995, ApJ 441, 96
Miller L., Goldschmidt P., La Franca F., Cristiani S., 1993, Observational Cosmology, eds. G. Chincarini, A. Iovino, T. Maccacaro, et al., ASP Conf. Ser. 51, 614
Miyaji T., Hasinger G., Schmidt M., 1998, in: Highlights in X-ray Astronomy, in press, astro-ph/9809398
Peacock J. A., 1983, MNRAS 202, 615
Reimers D., Wisotzki L., 1997, The Messenger 88, 14
Reimers D., Köhler T., Wisotzki L., 1996, A&AS 115, 235
Schmidt M., Green R. F., 1983, ApJ 269, 352
Schmidt M., Schneider D. P., Gunn J. E., 1995, AJ 110, 68
Schneider P., Ehlers J., Falco E.E., 1992, Gravitational Lenses, Springer-Verlag
Shaver P. A., Wall J. V., Kellerman K. I., Jackson C. A., Hawkins M. R. S., 1996, Nat 384, 439
Surdej J., Claeskens J.F., Crampton D., et al., 1993, AJ 105, 2064
Terrell J., 1977, Am. J. Phys. 45, 869
Turner E. L., 1980, ApJ 242, L135
Warren S. J., Hewett P. C., Osmer P. S., 1994, ApJ 421, 412
Wisotzki L., 1999, A&A, submitted
Wisotzki L., Köhler T., Groote D., Reimers D., 1996, A&AS 115, 227
Wisotzki L., Christlieb N., Bade N., et al., 1999, A&A, submitted (Paper 1)
Wolf C., Meisenheimer K., Röser H.-J., et al., 1999, A&A 343, 399